Raman Laser Switching Induced by Cascaded Light Scattering

Sho Kasumie, Fuchuan Lei, Jonathan M. Ward, Xuefeng Jiang, Lan Yang, and Síle Nic Chormaic**

It is shown that, in multimode Raman lasers, cascaded light scattering (CLS) not only extends the optical frequency range, but can also modulate the laser dynamics. The origin of this phenomenon lies in the fact that many Raman lasing modes are directly correlated through CLS. The coupled-mode equations only describe single-mode cascaded Raman lasers and are insufficient for describing the multimode case. In this work, additional terms are introduced to account for intermodal interaction and, therefrom the physical mechanism behind the mode-switching phenomenon is revealed. Additionally, mode-switching controlled solely by a single-mode pump in a whispering gallery mode (WGM) silica Raman laser is demonstrated. As the intracavity pump power is increased, laser switching happens between two adjacent WGMs in the same mode family.

1. Introduction

Stimulated light scattering, such as stimulated Raman scattering (SRS) and stimulated Brillouin scattering (SBS), can lead to the generation of coherent photons in different materials and geometries.[1,2] Unlike conventional inversion lasers, the emissions from stimulated-scattering lasers are not limited to specific wavebands since no real energy levels are required; this provides unique advantages in many applications, for example, arbitrary wavelength conversion,[3–5] high-quality microwave generation,[6] gyroscopes,[7] sensing,[8–13] mode control,[14,15] etc. Considering that the stimulated gain arises from coherent coupling between a pump field and a Stokes field mediated by another field, for example, a phonon field, the newly generated Stokes field may also act as a pump for the generation of further Stokes fields—an effect known as cascaded light scattering (CLS), resulting in cascaded Raman and Brillouin lasers.[16–20] Due to the presence of CLS, stimulated lasers are usually multimode when a high pump power is applied. Nevertheless, it is generally assumed that the dynamics of stimulated lasers involving CLS is trivial and usually attention is focused on the interactions of pump and Stokes waves. This is indeed true for Brillouin lasers because of the phase-matching condition.[19,21] However, in Raman lasers, as the phase matching condition is automatically satisfied[3] (see **Figure 1**a),[1] CLS could lead to many lasing modes being coupled together, hence rendering the behavior of such lasers to be quite unique, especially for multimode lasing.[22–24] As a specific example, here we show, both theoretically and experimentally, that CLS can induce mode-switching in multimode Raman lasers. This study illustrates the importance of considering CLS effects for Raman lasing in dielectric resonators.

In this work, a whispering gallery mode (WGM) silica Raman laser is chosen as the experimental platform.[25] As depicted in Figure 1b, the light fields can be coupled into and out of the WGM resonator through a waveguide. The Stokes light (i.e., the Raman laser) can be generated in a WGM resonator as long as the following requirements are met: i) the frequency of the Stokes light coincides with a high-Q WGM and ii) the Stokes mode has sufficient spatial overlap with the pump mode, in other words, mode overlap. With a single-mode pump, the Raman gain of a silica matrix can be considered to be homogeneously broadened if one neglects CLS (see Figure 1c). In this case, only the mode with the highest gain can lase, even if all the modes have the same losses, in other words, Q-factors, since the gain is clamped at the lasing threshold.[26] At this point, a question would naturally arise: how can one explain the frequent occurrence of multimode Raman lasing in a single-mode pumped microresonator?

Here, we show that, due to the existence of CLS, two (or multiple) modes with unequal gain provided by the pump, but equal cavity loss (more generally, unequal gain/cavity loss ratio) lase simultaneously (see Figure 1d). It is noteworthy to point out that this CLS-assisted multimode lasing scenario differs from

Dr. S. Kasumie, Dr. F. Lei, Dr. J. M. Ward, Prof. S. Nic Chormaic
Light-Matter Interactions for Quantum Technologies Unit
Okinawa Institute of Science and Technology Graduate University
Onna, Okinawa 904-0495, Japan
E-mail: fuchuan.lei@oist.jp; sile.nicchormaic@oist.jp

Dr. X. Jiang, Prof. L. Yang
Department of Electrical and Systems Engineering
Washington University
St. Louis, Missouri 63130, USA

Prof. S. Nic Chormaic
Université Grenoble Alpes
CNRS, Grenoble INP, Institut Néel, 38000 Grenoble, France

The ORCID identification number(s) for the author(s) of this article can be found under https://doi.org/10.1002/lpor.201900138

© 2019 The Authors. Published by WILEY-VCH Verlag GmbH & Co. KGaA, Weinheim. This is an open access article under the terms of the Creative Commons Attribution License, which permits use, distribution and reproduction in any medium, provided the original work is properly cited.

DOI: 10.1002/lpor.201900138

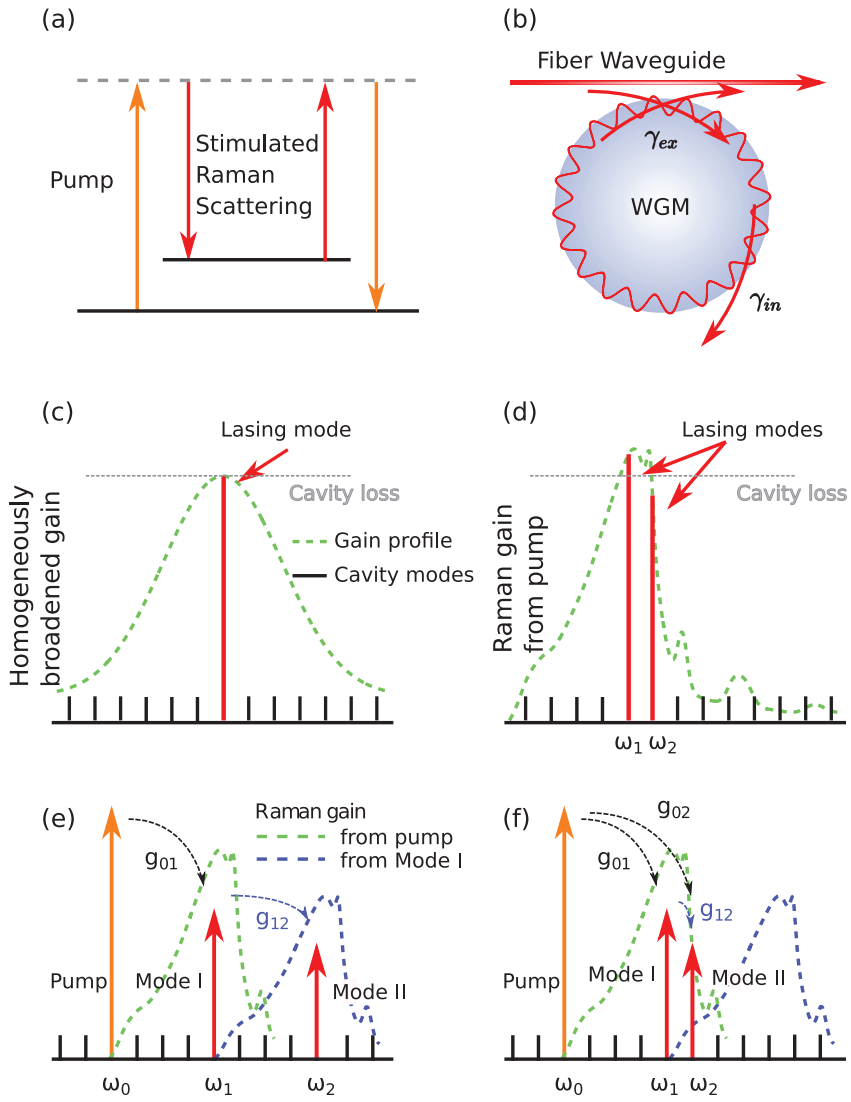


Figure 1. a) Schematic diagram of the stimulated Raman scattering process. b) Schematic of the experimental system. The input laser is coupled to a silica microsphere resonator through a tapered fiber waveguide, with a coupling constant, γ_{ex}, and resonator intrinsic loss, γ_{in}. c,d) Comparison of the gain spectrum and the lasing modes between a typical homogeneously broadened laser (c) and a silica Raman laser (d). e,f) Schematics of a cascaded Raman laser in single-mode fashion (e) and a two-mode Raman laser (f).

conventional cascaded single-mode Raman lasing, whereby a single mode is generated for each order of lasing, as shown in Figure 1e. The first order Raman lasing mode (Mode I), originating from the pump, could generate the subsequent Stokes field, that is, the second order Raman laser (Mode II), and the typical frequency shift between the pump and Stokes is about 14 THz. In this scenario, the pump does not provide gain directly to the second (or even higher order) Stokes field. Hence, the power of this Raman laser usually decreases with increasing order, and it is impossible to obtain a higher order Raman signal without the presence of its previous order. The dynamics of such a typical cascaded laser can be simply treated as a cascaded energy transfer process; therefore, it is trivial and does not differ much from the conventional single-mode lasing case. However, for the multimode lasing case, the presence of CLS can modulate the laser dynamics significantly. As illustrated in Figure 1f, two adjacent modes in the same mode family are excited simultaneously by a single-mode pump. Both Raman lasing modes derive their gain from the pump through SRS, but at the same time, the first Raman mode interacts with the second due to CLS. Though the interaction may be weak, it is not negligible and can account for the existence of multimode Raman lasing, and may even play a subtle role in Raman laser switching.

Indeed, the CLS-induced coupling between the two lasing modes seems not so obvious and is easily overlooked. In textbooks, the SRS is usually illustrated with two light fields and a simplified two level system, as shown in Figure 1a. However, in real solid materials, like silica,[27] silicon,[28] or silicon carbide,[29] the Raman gain profile is not simply composed of only a few discrete peaks, but rather is a continuum; therefore, it is natural to introduce a coupling term between the two lasing modes (see Figure 1f).

© 2019 The Authors. Published by WILEY-VCH Verlag GmbH & Co. KGaA, Weinheim

2. Theoretical Model

In order to understand the multimode Raman laser (see Figure 1f), here, the standard coupled-mode equations must be modified[16] to include *all* the CLS terms. Given a certain j^{th} cavity mode, it couples to the external driving pump in the waveguide via the overlap of the evanescent fields and to *all* the other cavity modes through SRS. We introduce a summation term into the coupled-mode equations to represent the interactions of the cavity modes. The motion of the intracavity field, E_j, can now be described as

$$\dot{E}_j = \left(-\frac{\gamma_j}{2} + \sum_{i<j} g_{ij}|E_i|^2 - \sum_{k>j} g_{jk}\frac{\omega_j}{\omega_k}|E_k|^2\right)E_j + \sqrt{\gamma_{ex,0}}\delta_{0j}s \quad (1)$$

where i, j, and k are mode order indices and the resonant frequencies decrease with the order (the order of the pump mode is set to be 0). The γ_j and $\gamma_{ex,j}$ denote the total energy decay rate and the extrinsic decay rate into the waveguide, respectively; ω_j is the resonant frequency; $I_0 = |s|^2$ is the input pump power from the waveguide; and δ is the Kronecker delta function, where $\delta_{ij} = 1$ if and only if $i = j$. We set g_{ij} as the intracavity Raman gain coefficient between mode i and j, proportional to the Raman gain spectrum of the bulk silica, $g_R(|\omega_i - \omega_j|)$.[27] Note that the Raman gain spectrum will not be modified due to the effect of cavity quantum electrodynamics (cQED).[30] The second and third terms in Equation (1) describe the gain and the loss caused by the SRS from the higher and lower frequency modes, respectively. It is important to point out that the coherent anti-Stokes Raman scattering is not included in the model since the phase-matching condition is not easily satisfied, as discussed later.

In order to gain insight into this phenomenon, we consider the simplest case of having a single pump mode and two Raman lasing modes (see Figure 1f). The intracavity powers for steady-state are governed by

$$P_0\left(-\frac{\gamma_0}{2} - g_{01}\frac{\omega_0}{\omega_1}P_1 - g_{02}\frac{\omega_0}{\omega_2}P_2\right)^2 = \gamma_{ex,0}I_0 \quad (2)$$

$$P_1\left(-\frac{\gamma_1}{2} + g_{01}P_0 - g_{12}\frac{\omega_1}{\omega_2}P_2\right) = 0 \quad (3)$$

$$P_2\left(-\frac{\gamma_2}{2} + g_{02}P_0 + g_{12}P_1\right) = 0 \quad (4)$$

where P_0, P_1, and P_2 represent the intracavity power for the pump, the first (Mode I), and the second (Mode II) lasing mode, respectively. There are four different steady-state regimes as I_0 is increased, see **Figure 2**a,b. Mode I is located in the vicinity of the peak of the Raman gain profile, while Mode II has a lower resonant frequency and a relatively lower Raman gain coefficient. Therefore, Mode I lases first, as long as its gain can overcome its loss (regime II), as shown in Figure 2a,b. One can see that P_1 continues to increase with I_0, but the intracavity pump power, P_0, is clamped at $\gamma_1/2g_{01}$. Thus, Mode II cannot derive sufficient gain solely from the pump field to start lasing. However, as shown in Figure 2b, Mode I can also provide a gain mechanism for Mode

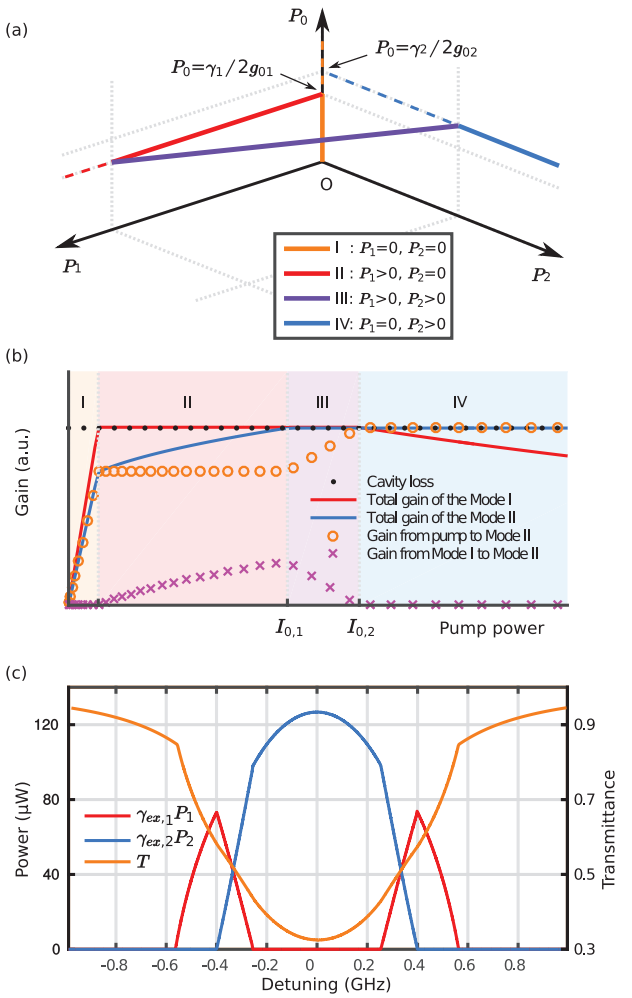


Figure 2. Simulation results based on Equation (1). a) P_0, P_1, and P_2 represent the intracavity powers of the pump, the first, and the second Raman fields. The external pump power is increased when detuning is set to 0. Solid lines represent the stable, steady state, while the dashed lines correspond to unstable cases. b) The total gain of the two Raman modes and gain fraction from the pump and Mode I to Mode II. c) The output of two Raman lasers and the transmission spectrum (T) of the pump mode as it evolves with pump detuning. The parameters used in (b) and (c) are: $\gamma_j = 25.3\ \mu s^{-1}$ and $\gamma_{ex,j} = 26.2\ \mu s^{-1}$ for all $j = 0, 1, 2$; the input power in (c) is fixed as $I_0 = 0.6$ mW; the angular frequencies are $\omega_0 = 2\pi \times 390.6$ THz, $\omega_1 = 2\pi \times 377$ THz and $\omega_2 = 2\pi \times 375.3$ THz; the intracavity Raman gain coefficients are $g_{01} = 3.6 \times 10^{18}\ s^{-1}J^{-1}$, $g_{02} = 2.7 \times 10^{18}\ s^{-1}J^{-1}$ and $g_{12} = 0.5 \times 10^{18}\ s^{-1}J^{-1}$, estimated based on ref. [27]

II proportional to P_1; the second mode can be excited and the system undergoes a transcritical bifurcation when

$$I_{0,1} = \frac{\gamma_1}{8\gamma_{ex,0}g_{01}}\left[\gamma_0 + \frac{1}{g_{12}}\frac{\omega_0}{\omega_1}(g_{01}\gamma_2 - g_{02}\gamma_1)\right]^2 \quad (5)$$

which can be obtained by setting $P_2 = 0$ and $-\gamma_2/2 + g_{02}P_0 + g_{12}P_1 = 0$ in Equations (2)–(4).

As a consequence of the appearance of Mode II (regime III), Mode I is gradually suppressed, since the former opens a loss path for the latter through SRS,[1] with the loss being proportional

© 2019 The Authors. Published by WILEY-VCH Verlag GmbH & Co. KGaA, Weinheim

to P_2. When two Raman modes lase simultaneously, P_1 and P_2 are determined from a simple linear relationship

$$g_{01}P_1 + g_{02}\frac{\omega_1}{\omega_2}P_2 = \frac{(g_{01}\gamma_2 - g_{02}\gamma_1)}{2g_{12}}. \quad (6)$$

Clearly, both modes are still influenced by I_0. In the two-mode lasing regime, the intracavity pump power, P_0, increases with I_0, while P_1 reduces with I_0 until

$$I_{0,2} = \frac{\gamma_2}{8\gamma_{ex,0}g_{02}}\left[\gamma_0 + \frac{1}{g_{12}}\frac{\omega_0}{\omega_1}(g_{01}\gamma_2 - g_{02}\gamma_1)\right]^2 \quad (7)$$

where Mode I is completely switched off (see Figure 2a,b). Even with further increasing of the pump, Mode I cannot be turned on again and only Mode II remains on (regime IV). This counter-intuitive phenomenon can be explained by considering the following two aspects: First, the existence of Mode II reduces the Q-factor of Mode I, and the threshold of Mode I increases with P_2; secondly, the gain provided to Mode I is fixed because Mode II causes the intracavity pump power to be clamped. The latter has no correspondence with conventional cascaded single-mode Raman lasers. Therefore, the mode switching induced by CLS cannot be readily illustrated as a unidirectional energy transfer between two lasing modes; in fact, it implies that the weak mode interaction could modulate the lasing dynamics of multimode lasers dramatically.

It is worth mentioning that there is no hysteresis phenomenon when the pump power, I_0, is ramped down; hence, it is possible to control the lasing modes simply by changing I_0. It is convenient to control the intracavity power, P_0, by changing the relative detuning of the pump and cavity modes; therefore, we perform numerical calculations for the scanning pump case, as shown in Figure 2c. It turns out that the four regimes can be achieved by controlling the detuning. As the detuning decreases, Mode I is excited first. Further detuning simultaneously turns on Mode II and suppresses Mode I. When the system is operated close to resonance, Mode I is annihilated completely and Mode II keeps growing until maximum coupling is reached.

3. Experimental Results

To experimentally confirm the mode switching, we performed measurements using a silica microsphere with a diameter of around 41.5 µm, fabricated from standard optical fiber reflowed by a CO_2 laser.[31] A tapered optical fiber was used to couple the pump light into the cavity through evanescent coupling (see Figure 1b). The output laser was divided into two paths, one for observing the transmission spectrum of the WGM resonator and the other for observing the Raman lasing spectrum. The transmission spectrum was recorded using a photodiode connected to a digital oscilloscope and was used for locking the pump to the WGM. The Raman lasing spectrum was measured by an optical spectrum analyzer (OSA). To avoid parametric oscillation and coherent anti-Stokes Raman scattering, the pump wavelength was set to 768.1 nm—this corresponds to the normal dispersion regime for silica.[32,33] The input laser power was approximately 500 µW and the laser frequency was finely tuned and thermally

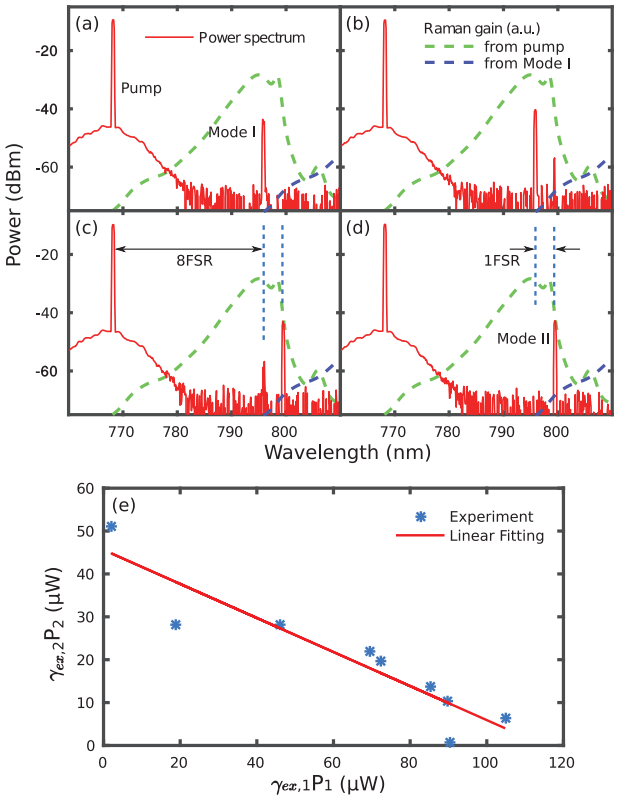


Figure 3. The switching process of the Raman lines is observed by scanning the pump laser in the blue-detuned region of a cavity mode at 768.1 nm. From (a) to (d), the detuning of the pump is approximately set at 20, 18, 15, and 10 MHz, respectively. a) The first Raman laser at 795.9 nm appears (Mode I). b) The second Raman line (Mode II) at 799.4 nm appears. c) Mode I is suppressed while Mode II becomes stronger. d) Mode I is annihilated and only Mode II remains. e) The output powers of Mode I and Mode II are negatively and linearly correlated with each other.

locked to a cavity mode[34] with a Q-factor of 9.7×10^7. During the thermal locking process, both the pump and lasing modes were red shifted; thus, their frequency intervals remain nearly unchanged and the change of the Raman gain can be negligible as well.

The experimental results are presented in **Figure 3**. As the laser frequency approaches resonance, the first Raman lasing mode (Mode I) at 795.9 nm is excited, with its power increasing as the detuning decreases until the second Raman lasing mode (Mode II) at 799.4 nm appears. With a further reduction of the detuning, power switching between the two Raman modes is observed and, eventually, only Mode II remains on, as evidenced in Figure 3d. The output powers of both Mode I and Mode II during the switching process were measured and are plotted in Figure 3e.

The powers of these two lasing modes are negatively and linearly correlated with each other during the switching process, in qualitative agreement with the theoretical model (see in Figure 2a) and Equation (6)). Note that the frequency spacings between the pump and two lasing modes are exactly integer numbers of the free spectral range (FSR), so they belong to the same mode family and, therefore, have near unity mode overlap. Otherwise, overlap coefficients would need to be introduced into Equa-

© 2019 The Authors. Published by WILEY-VCH Verlag GmbH & Co. KGaA, Weinheim

tion (1). The mode overlap is particularly important for a standing wave resonator in which the Raman gain saturation could intrinsically lead to stable, single-mode lasing at a high power.[35] This is because the CLS may be suppressed due to weak mode overlap as it may simply be too small to allow CLS to occur.

In these experiments, we selected resonators with a low number of high-Q modes to avoid an overly complicated WGM spectrum and to reduce the chance of cascaded lasing beyond the first order. When we used an even higher pump power, or a smaller detuning, many high order cascaded lasing modes (up to at least 11 modes) were often observed. In some samples, we also observed the conventional cascaded lasing modes in single-mode fashion before the appearance of the second Raman lasing modes in the first order. This can be attributed to the differences in the Q-factors and the FSR for different resonators. There is an abundance of switching behaviors due to CLS when multiple lasing modes are involved; this is especially true when the phase-matching condition is satisfied and other nonlinear optical phenomena occur simultaneously. Detailed analysis of these sophisticated processes are beyond the scope of this work.

4. Summary

In summary, although a lot of interest has been garnered, and many applications have been demonstrated, few studies have focused on understanding the details of cascaded light scattering in Raman lasers. In this work, we show that, aside from the application for extending the frequency range, naturally occurring CLS has a significant impact on the generation of Raman lasing and cannot be ignored when multiple modes are involved. Subsequently, it may have an impact on the realization of Kerr-frequency combs,[36–40] phase-locked Raman lasers,[37,41] and soliton generation.[42–44] Besides Raman lasers, this SRS interaction also exists in other lasers, such as rare-earth-doped microlasers; hence, the mode switching induced by SRS could provide a strategy to achieve a wavelength-switchable laser via CLS in a variety of laser systems. Exploring this dynamically related phenomenon[45,46] may find direct applications in all-optical, flip-flop memories[47] and switchable light sources.

Acknowledgements

S.K. and F.L. contributed equally to this work. This work was supported by the Okinawa Institute of Science and Technology Graduate University (OIST).

Conflict of Interest

The authors declare no conflict of interest.

Keywords

cascaded light scattering, mode switching, Raman lasers, whispering gallery modes

Received: April 23, 2019
Revised: August 11, 2019
Published online:

[1] R. W. Boyd, *Nonlinear Optics*, Elsevier, Amsterdam, The Netherlands **2003**.
[2] G. Lin, A. Coillet, Y. K. Chembo, *Adv. Opt. Photonics* **2017**, *9*, 828.
[3] S. M. Spillane, T. J. Kippenberg, K. J. Vahala, *Nature* **2002**, *415*, 621.
[4] O. Boyraz, B. Jalali, *Opt. Express* **2004**, *12*, 5269.
[5] H. Rong, A. Liu, R. Jones, O. Cohen, D. Hak, R. Nicolaescu, A. Fang, M. Paniccia, *Nature* **2005**, *433*, 292.
[6] J. Li, H. Lee, K. J. Vahala, *Nat. Commun.* **2013**, *4*, 2097.
[7] J. Li, M.-G. Suh, K. Vahala, *Optica* **2017**, *4*, 346.
[8] X. Jiang, A. J. Qavi, S. H. Huang, L. Yang, arXiv:1805.00062, **2018**.
[9] S. K. Ozdemir, J. Zhua, X. Yangb, B. Penga, H. Yilmaza, L. Hea, F. Monifia, S. H. Huanga, G. L. Longb, L. Yang, *Proc. Natl. Acad. Sci. USA* **2014**, *111*, E3836.
[10] X.-F. Jiang, Y.-F. Xiao, Q.-F. Yang, L. Shao, W. R. Clements, Q. Gong, *Appl. Phys. Lett.* **2013**, *103*, 101102.
[11] G. Zhao, Ş. K. Özdemir, T. Wang, L. Xu, E. King, G.-L. Long, L. Yang, *Sci. Bull.* **2017**, *62*, 875.
[12] B.-B. Li, W. R. Clements, X.-C. Yu, K. Shi, Q. Gong, Y.-F. Xiao, *Proc. Natl. Acad. Sci. USA* **2014**, *111*, 14657.
[13] Y. Chen, Z.-H. Zhou, C.-L. Zou, Z. Shen, G.-C. Guo, C.-H. Dong, *Opt. Express* **2017**, *25*, 16879.
[14] X. Yang, Ş. K. Özdemir, B. Peng, H. Yilmaz, F.-C. Lei, G.-L. Long, L. Yang, *Opt. Express* **2015**, *23*, 29573.
[15] Y. H. Wen, O. Kuzucu, M. Fridman, A. L. Gaeta, L.-W. Luo, M. Lipson, *Phys. Rev. Lett.* **2012**, *108*, 223907.
[16] B. Min, T. J. Kippenberg, K. J. Vahala, *Opt. Lett.* **2003**, *28*, 1507.
[17] T. J. Kippenberg, S. M. Spillane, B. Min, K. J. Vahala, *IEEE J. Sel. Top. Quantum Electron.* **2004**, *10*, 1219.
[18] H. Rong, S. Xu, O. Cohen, O. Raday, M. Lee, V. Sih, M. Paniccia, *Nat. Photonics* **2008**, *2*, 170.
[19] I. S. Grudinin, A. B. Matsko, L. Maleki, *Phys. Rev. Lett.* **2009**, *102*, 043902.
[20] G. Lin, S. Diallo, K. Saleh, R. Martinenghi, J.-C. Beugnot, T. Sylvestre, Y. K. Chembo, *Appl. Phys. Lett.* **2014**, *105*, 231103.
[21] M. Tomes, T. Carmon, *Phys. Rev. Lett.* **2009**, *102*, 113601.
[22] L. Ge, D. Liu, A. Cerjan, S. Rotter, H. Cao, S. G. Johnson, H. E. Türeci, A. D. Stone, *Opt. Express* **2016**, *24*, 41.
[23] H. A. M. Leymann, D. Vorberg, T. Lettau, C. Hopfmann, C. Schneider, M. Kamp, S. Höfling, R. Ketzmerick, J. Wiersig, S. Reitzenstein, A. Eckardt, *Phys. Rev. X* **2017**, *7*, 021045.
[24] N. Zhang, Y. Fan, K. Wang, Z. Gu, Y. Wang, L. Ge, S. Xiao, Q. Song, *Nat. Commun.* **2019**, *10*, 1770.
[25] J. Ward, O. Benson, *Laser Photonics Rev.* **2011**, *5*, 553.
[26] J. T. Verdeyen, in *Laser Electronics*, 2nd ed., Prentice Hall, Englewood Cliffs, NJ, USA **1989**, p. 640.
[27] D. Hollenbeck, C. D. Cantrell, *J. Opt. Soc. Am. B* **2002**, *19*, 2886.
[28] K. Uchinokura, T. Sekine, E. Matsuura, *Solid State Commun.* **1972**, *11*, 47.
[29] P. J. Colwell, M. V. Klein, *Phys. Rev. B* **1972**, *6*, 498.
[30] A. Matsko, A. Savchenkov, R. Letargat, V. Ilchenko, L. Maleki, *J. Opt. B: Quantum Semiclass. Opt.* **2003**, *5*, 272.
[31] R. M. Murphy, F. Lei, J. M. Ward, Y. Yang, S. Nic Chormaic, *Opt. Express* **2017**, *25*, 13101.
[32] D. Farnesi, F. Cosi, C. Trono, G. C. Righini, G. N. Conti, S. Soria, *Opt. Lett.* **2014**, *39*, 5993.
[33] I. H. Agha, Y. Okawachi, M. A. Foster, J. E. Sharping, A. L. Gaeta, *Phys. Rev. A* **2007**, *76*, 043837.
[34] T. Carmon, L. Yang, K. J. Vahala, *Opt. Express* **2004**, *12*, 4742.
[35] O. Lux, S. Sarang, O. Kitzler, D. J. Spence, R. P. Mildren, *Optica* **2016**, *3*, 876.
[36] R. Suzuki, A. Kubota, A. Hori, S. Fujii, T. Tanabe, *J. Opt. Soc. Am. B* **2018**, *35*, 933.

© 2019 The Authors. Published by WILEY-VCH Verlag GmbH & Co. KGaA, Weinheim

[37] W. Liang, V. Ilchenko, A. Savchenkov, A. Matsko, D. Seidel, L. Maleki, *Phys. Rev. Lett.* **2010**, *105*, 143903.
[38] Y. Okawachi, M. Yu, V. Venkataraman, P. M. Latawiec, A. G. Griffith, M. Lipson, M. Lončar, A. L. Gaeta, *Opt. Lett.* **2017**, *42*, 2786.
[39] T. Kato, A. Hori, R. Suzuki, S. Fujii, T. Kobatake, T. Tanabe, *Opt. Express* **2017**, *25*, 857.
[40] A. Cherenkov, N. Kondratiev, V. Lobanov, A. Shitikov, D. Skryabin, M. Gorodetsky, *Opt. Express* **2017**, *25*, 31148.
[41] G. Lin, Y. K. Chembo, *Opt. Lett.* **2016**, *41*, 3718.
[42] T. Herr, V. Brasch, J. D. Jost, C. Y. Wang, N. M. Kondratiev, M. L. Gorodetsky, T. J. Kippenberg, *Nat. Photonics* **2014**, *8*, 145.
[43] M. Karpov, H. Guo, A. Kordts, V. Brasch, M. H. P. Pfeiffer, M. Zervas, M. Geiselmann, T. J. Kippenberg, *Phys. Rev. Lett.* **2016**, *116*, 103902.
[44] Q.-F. Yang, X. Yi, K. Y. Yang, K. Vahala, *Nat. Phys.* **2017**, *13*, 53.
[45] S. V. Zhukovsky, D. N. Chigrin, A. V. Lavrinenko, J. Kroha, *Phys. Rev. Lett.* **2007**, *99*, 073902.
[46] F. Lei, Y. Yang, J. M. Ward, S. Nic Chormaic, *Opt. Express* **2017**, *25*, 24679.
[47] L. Liu, R. Kumar, K. Huybrechts, T. Spuesens, G. Roelkens, E.-J. Geluk, T. De Vries, P. Regreny, D. Van Thourhout, R. Baets, G. Morthier, *Nat. Photonics* **2010**, *4*, 182.

© 2019 The Authors. Published by WILEY-VCH Verlag GmbH & Co. KGaA, Weinheim